Electrically Improving a MEMS Sensor for Rolling Stock

James P. Hofmeister, Wyatt Pena, Erik Sandberg, and Robert S. Wagoner
Ridgetop Group, Inc.
3580 West Ina Road
Tucson, AZ 85741
520-742-3300
jhofmeister@ridgetopgroup.com

Abstract: This paper describes work related to improving the electrical performance of an accelerometer-based sensor, RotoSense™, used for monitoring rolling stock: the locomotives and cars used in trains. At the 2018 MFPT conference, a paper, "Improved RotoSense™ for Rolling Stock: Locomotives and Cars," focused on physical improvements to the shaft-mounted, wireless sensor, although there were improvements in signal performance. This paper describes subsequent improvements to that sensor, with focus on signal quality and battery life. The original version of the sensor described in this paper is the first and, still, only known to survive, intact, three days of testing at the National Test Track Center in Pueblo, Colorado, including a 10-hour, non-stop, 400-mile test run. The rationale, the methods, and the results of those electrical improvements are the focus of this paper.
*RotoSense is a trademark of Ridgetop Group, Inc.

Keywords: Accelerometer; gear; MEMS; rolling stock; RotoSense, signal quality; train, wheel hub

1. INTRODUCTION

Equipment such as robots and gear boxes that incorporate rotating shafts often need to monitor rotational vibration and shaft speed, as part of broader condition-based maintenance (CBM) systems. Fault detection equipment on drive systems typically use accelerometers mounted on transmission housings to capture, measure, and process vibration signals. The usefulness and flexibility of such detection equipment for applications involving rotating shafts, including pinion and planetary gears, have been limited by cabling, slip-ring approaches, and multiple sensors to obtain monitoring information. For more complex systems, especially those with poor signal transmission paths, a shaft-mounted, wireless solution based on a micro-electro-mechanical system (MEMS) is needed (see Figure 1) [1] [2] [3] [4].

A prototype solution was designed, developed, and imbedded on a rotating shaft used in helicopter transmissions to capture and measure vibration signals, and then a MEMS version mounted on the wheel hubs of rolling stock was developed.

This paper focuses on the methodology and results in ruggedization, improved signal quality, and increased battery life of those solutions.

2. Theoretical Background

MEMS-based accelerometers that measure acceleration and force, such as produced by vibration and shock, were used in prototype solutions for the following applications: (1) mounting inside helicopter transmissions and (2) mounting on the hubs of rolling stock of trains to detect features of railroad tracks.

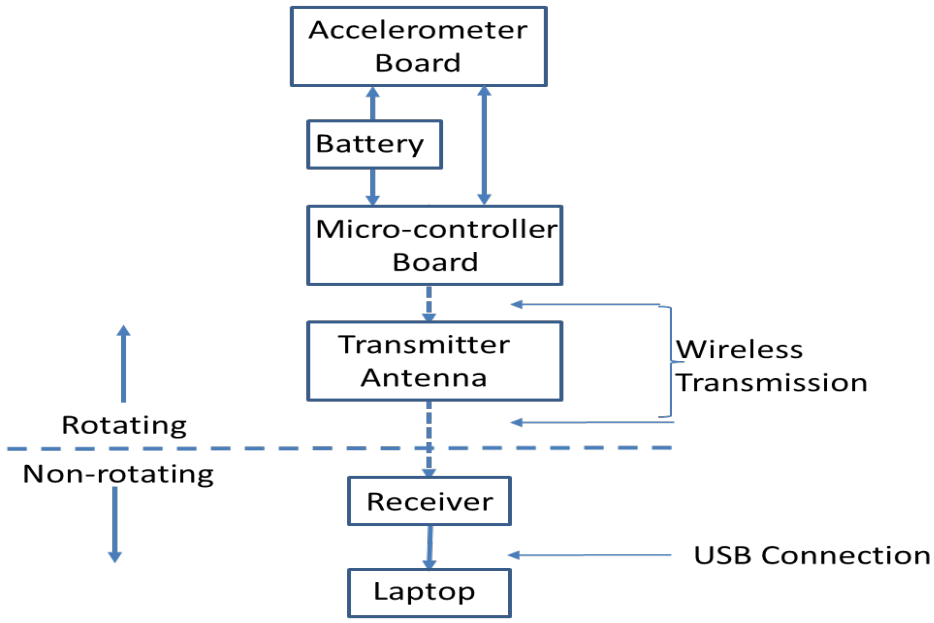

Figure 1: Simple MEMS Block Diagram. [2]

Helicopter Transmission: Pinion Gear

A specific application was the spiral-bevel pinion of an OH-58C transmission (see Figure 2). For that application, MEMS Sensing Package was designed and developed to contain a microcontroller board, an accelerometer board, and a battery pack mounted in a cylindrical canister (Figure 3).

A NASA Glenn Research Center, Small Business Innovation Research (SBIR) award led to an experiment in which a tooth on the spiral bevel gear was pre-notched and then the transmission was run to tooth failure. The feasibility of shafted-mounted solutions was proven comparable to traditional stationary, housing mounted accelerometer solutions.

Wheel Hubs of Rolling Stock

Figure 4 (left) shows the physical adaptation of the MEMS-based sensor for mounting on wheel hubs of the shafts of the trucks of train locomotives and cars. This version of the sensor was designed and developed to prove feasibility for using such sensors to locate and

identify anomalies related to railroad tracks. The adapted system for rolling stock applications comprises a MEMs sensor and a gateway to collect data and write data to disk storage as files. The MEMS sensors were mounted on wheels of a train to produce shock data during test runs of a train over a High Tonnage Loop (HTL) test track (TT) to process the data, identify high-force events (HFEs), and locate the position on the HTL TT where HFEs occurred. The purpose was to demonstrate/validate an ability to support focused inspection of tracks to identify and locate anomalies requiring monitoring and service [2].

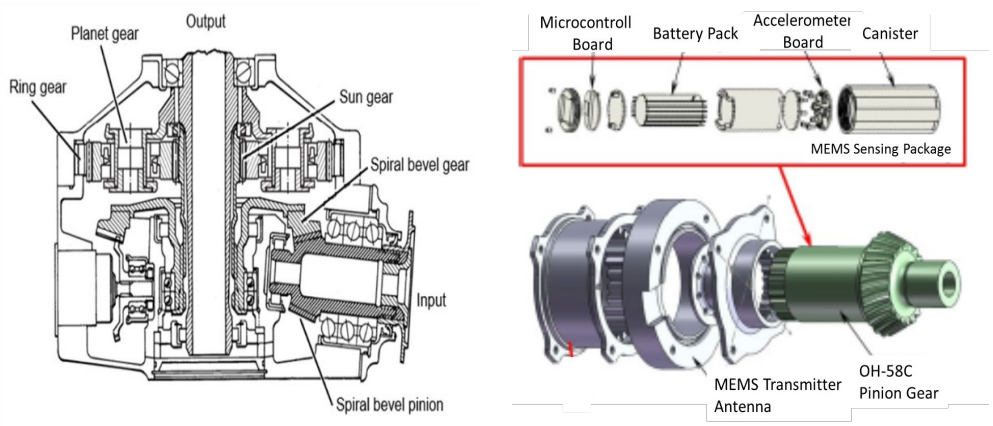

Figure 2: OH-58C Transmission (Left) and RotoSense on the Pinion Gear (Right).

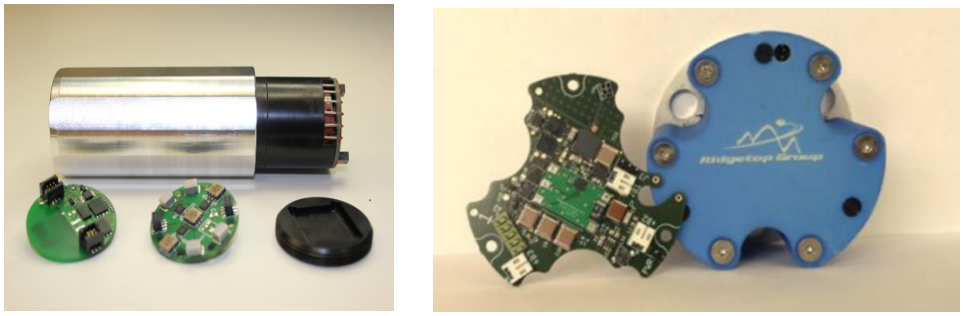

Figure 3: Canister, Boards, End Cap (Left) and Boards w/Batteries and Housing (Right).

Initial Results: Shaft-mounted, beveled-pinion gear

A RotoSense configuration of triple shaft-mounted sensors were installed on pre-notched OH-58C spiral-bevel pinion gears and endurance tests at NASA's Glenn Research Center were performed and run to tooth fracture failure: the notch was extended at run time = 51.9 hours and widened at run time = 106 hours (Figure 4, right).

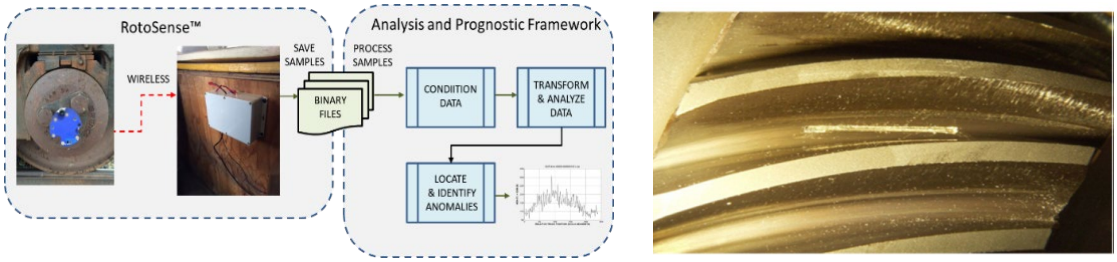

Figure 4: Rolling-stock Sensor System (Left) and Final Gear-Tooth Notching (Right).

The sensors performed well, lasted the entire test, and all MEMS accelerometers gave an indication of failure at the end of the test. The MEMS systems performed as well, if not better than, the existing stationary accelerometers mounted on the gear box housing with regards to gear tooth fault detection (Figure 5, left) and time-synchronous-average (TSA) signals (Figure 5, right) [1].

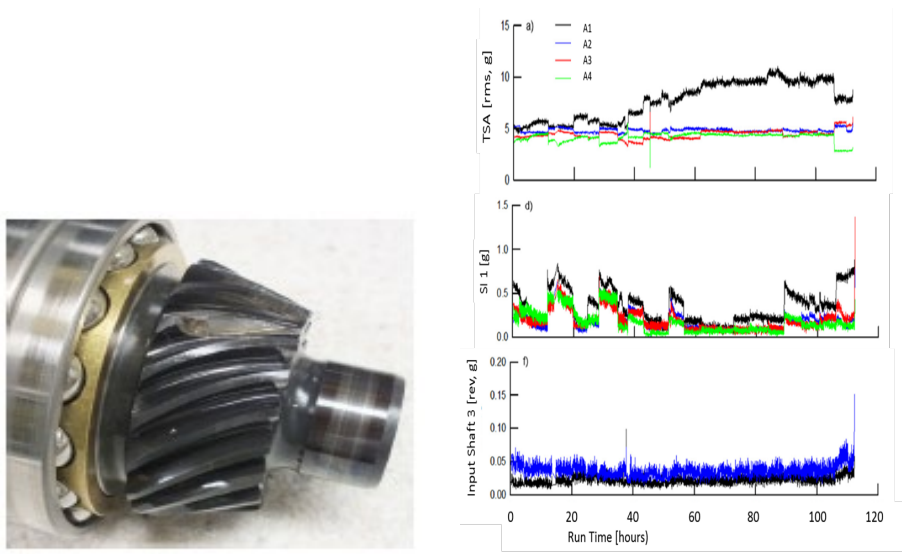

Figure 5: Fractured-Tooth Failure (Left) and Data (Right).

For both the MEMS sensors and stationary sensors, the fault detection time was not much sooner than the actual tooth fracture time. The MEMS sensor spectrum data showed large first-order shaft frequency sidebands due to the measurement rotating frame of reference. The method of constructing a pseudo tach signal from periodic characteristics of the vibration data was successful in deriving TSA signals without an actual tachometer: the method proved to be an effective way to improve fault detection for the MEMS [1].

Initial Results: Hub-mounted, freight car of a train

The configuration for train applications includes RotoSense, a MEMS sensor, supporting firmware and software to support collecting, wireless transmitting of data to a gateway, and saving data in binary files. The assemblies are mounted to the wheel hubs to rotate with the axle so any anomalies in the wheels or track can be detected (see Figure 8).

MEMS Configuration

The MEMS is configured as a three-axis accelerometer with 57mV/g sensitivity with a 158 Hz sampling rate: sensor was mounted concentrically on each end of a freight car axle and also on a locomotive axle of a train, as shown in Figure 6.

Figure 6: RotoSense – Wheel-Hub Mounted.

Test Train, Track, and Train Movement

Test Train: A test train at the National Test Track Center at Pueblo, Colorado, comprised three (3) locomotives and 110 freight cars and was run on a high-tonnage loop (HTL) test track (TT) used for research under heavy axle-loads to test track-component reliability, wear, and fatigue.

Test Track: The HTL track length is 2.7 miles divided into test sections that generally correspond to tangents, spirals, curves, and turnouts that are populated with features and test sections as seen in Figure 7. Table 1 lists the TT features and Figure 8 and Figure 9 show some of features listed in Table 1.

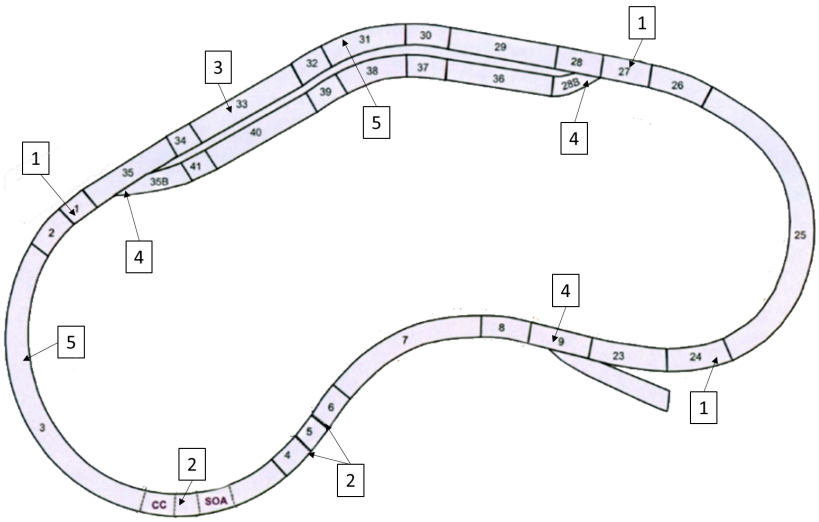

Figure 7: Layout of the Heavy Tonnage Loop Test Track.

Table 1: Key Physical Features of the HTL TT Shown in Figure 11.

1. Lubricator	2. Steel Bridge	3. Crib Ties and Fasteners
4. 405, 407 or 408 turnout and frog or switch	5. Thermite or Overlay Welds	6. Concrete Bridge

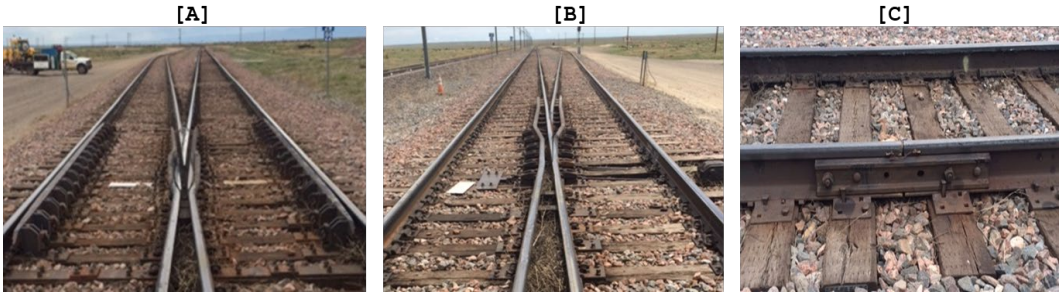

Figure 8: Turnout and Frog, Switch left [A] and Switch Right [B]; Steel Bridge [C].

Figure 9: Concrete Bridges [A] & Bot of [B]; Crib Ties @ Top of [B].

Train Movement: The train was auto-controlled to run 15 laps per hour: 4 minutes per lap and 38,640 samples per lap. Four test runs were started on four days (May 11 – May 14 in 2015). Table 2 summarizes the May 14 test run from 2000 to 0632 the next morning: 10 hours, 32 minutes and over 4 million sets of six-byte data. The train started to move about 30 minutes after the sensors were turned on: the train was moved to the test track and two laps of test conditioning were run. After that, the train was kept at a constant speed of 15 laps per hour (4-minute laps).

Data Collection and Analysis

Test Data: Data was collected and buffered for each axis at a sampling rate of 158 Hz and the buffered data was transmitted to a collection hub and saved in output files about once every 1.11 seconds. The data was analyzed, nominal values determined for zero-force conditions, and transformed into +/- values with respect to zero-force.

Data Analysis: Data analysis was hampered by the loss of Global Positioning Data (GPS) caused by a broken antenna. Consequently, raw data (Figure 10, left) was analyzed by binning the data in terms of magnitude (xy-plane, the z-plane, and both planes) and relative laps (Figure 10, right), examining the peaks, and comparing those peaks to features of the test track: pattern matching.

Table 2: Summary of the Test Run Started on May 14, 2015.

Description			**Comments**
Train	3 locomotives 110 cars		6,780' long (1.3 miles). Hopper car lengths, coupler to coupler, range from ~58.5 to 60.5 feet: used 60-foot length.
Build	92 minutes		2000 start; 2132 completed build
Run	540 minutes	132 laps	2132: started test conditioning run (TCR)
	17 minutes	2 laps	2149: completed TCR
	518 minutes	129 laps	2149 – 0627: testing
	5 minutes	1 lap	0632: end of test
Wheel 1	20645 files		
Wheel 4	20565 files		

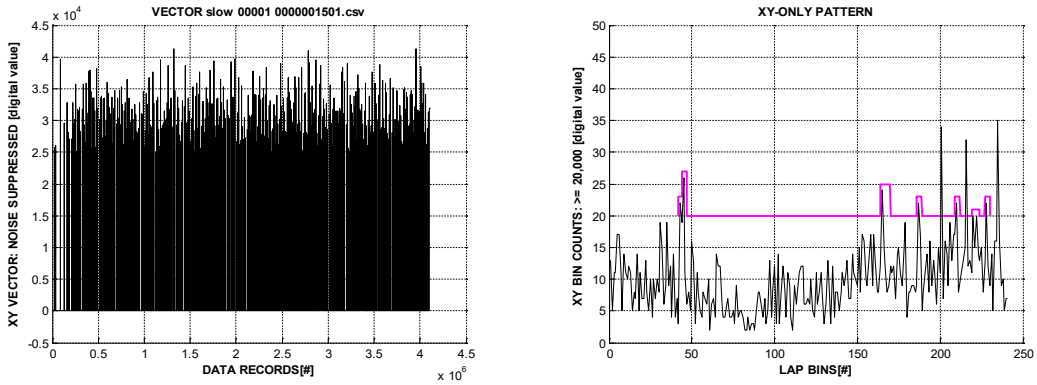

Figure 10: XY-plane Data, Raw (Left) and Binned by Bin Number, Right).

We successfully proved that, even without GPS, we were able to synchronize the data to the start of the test track and then locate those features that could be located: as seen indicated in Figure 11 and Table 3.

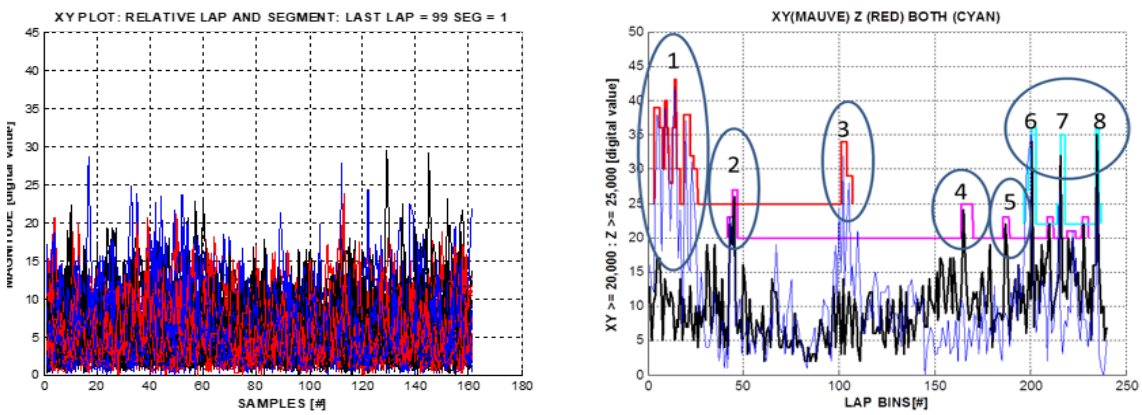

Figure 11: Data & Identified Features (1) Through (8) of Table 3.

Table 3: TT Description and Detection Evaluation.

Track Sections	Feature Sections	TT ID	Track Feature	Detection Evaluation	
				XY-vector	Z-vector
1 – 3		S1	Lubricator	ND	ND
4 – 5		S2			
6 - 62	5-26	S3	Repair/overlay welds		Yes (1)
	30-40	S3	Concrete bridge	Maybe	maybe
	42-46	S3	Concrete bridge	Maybe	Yes (2)
63 – 66		S4	Steel bridges	ND	ND
67 – 69		S5	Bridge deflection	ND	ND
70 – 73		S6	Steel bridges	ND	ND
74 – 92		S7	Rail performance	ND	ND

93 – 97		S8	Fiber optic cable	ND	ND
98 – 108		S9	405 turnout/frog		Yes (3)
109 - 117		S23	405 turnout/frog		Yes (3)
118 – 125		S24	Lubricator	ND	ND
126 – 163		S25	TPO, Tie and fastener, performance	Yes (4)	No
164 – 170		S26			
171 – 175		S27	Lubricator	ND	ND
176 – 180		S28	Turn out, steering switch, foundation	Yes (5)	
181 – 193		S29	LTM Tests	ND	ND
194 – 198		S30			
199 – 208		S31	FRA: Rail-seat deterioration, Thermite welds	Yes (6)	Yes (6)
209 – 212		S32			
213 – 225		S33	Crib ties	Yes (7)	Yes (7)
226 – 229		S34			
230 - 240		S35	407 turnout/frog	Yes (8)	Yes (8)

Note: ND means Not Detectable.

3. METHODOLOGY: RUGGEDIZATION, SIGNAL QUALITY, AND BATTERY LIFE

Subsequently, a manufacturer of rolling stock obtained sensor units and software and performed additional testing and evaluation. The units were found deficient because of the following: (1) physical failure at high-force testing at 40 g vibration and shock leading to board flexing and subsequent solder joint failures and battery displacement; (2) inaccurate vibrational readings caused by flexing of the printed circuit boards.

Operational concerns were reported in the following areas: (1) communication setup between the Sentinel Gateway and Laptop; (2) communication setup between RotoSense sensor and Sentinel Gateway; (3) sending commands to the RotoSense sensor; and (4) setting a synchronized time on a RotoSense sensor.

An improved MEMS-based sensor (Figure 12) was developed using the following approaches: (1) employ potting; (2) reposition the PCB board and the battery; (3) improve

the quality of the built assembly to ensure an ability to withstand stresses and flexing due to high-g vibration and shock; and (4) operational design changes to reduce power consumption and thereby improve battery life.

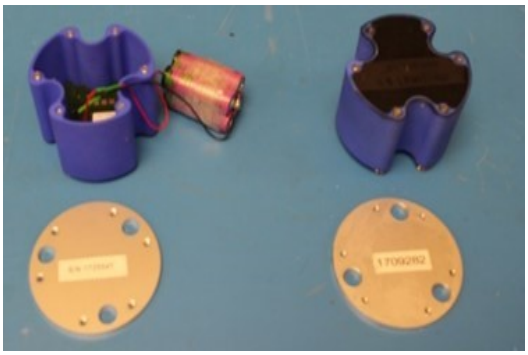

Figure 12: Original (Left) and Improved (Right) Sensors

Quality improvements included inspections and procedures regarding use, assembly, and testing. Improvements included hardware, software solutions, and documentation.

Final testing of the improved MEMS-based sensor, was performed at the National Technical Systems (NTS) test facilities in Tempe, Arizona and at Ridgetop Group laboratories in Tucson, Arizona.

Epoxy-based Potting

An epoxy-based potting was employed: (1) prevented battery displacement; (2) PCB protection from internal vibration and shock forces; (3) increased accuracy in sensor readings; and reduction of additional internal forces. Experiments were performed on sensor units with no potting, partial potting, and full potting. Partial and full potting addressed battery displacement, but partial potting did not fully address board flexing: full potting yielded the best results: zero defects related to shock and vibration occurred during initial and final testing conducted at Ridgetop Group and at NTS.

Component Repositioning

Experiments were performed using variations of component placement: the highest quality signals were obtained using the component placement shown in Figure 13.

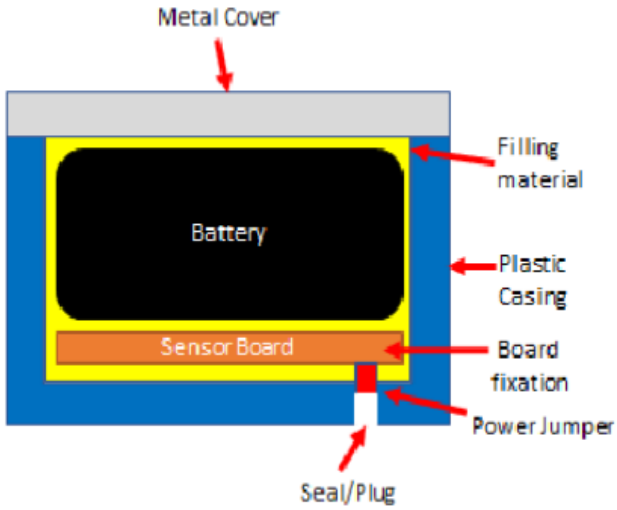

Figure 13: Component Placement Diagram.

Software and Firmware Improvement

Supporting software updates include an updated file structure for more flexible control of future parameter changes. Firmware updates include the following:

1. Updated sensor-gateway communications
2. Updated gateway firmware to reduce timeouts
3. Sensor firmware, functional improvements:
    - Ability to change sensor node address
    - Ability to change the computer IP address to which the data is transmitted
    - Set time on sensors
    - Read sensor temperature
    - Read radio frequency
    - Improved the wireless speed capabilities from 5.5KB/S to 11KB/S.

Documentation Improvement

The documentation was improved as follows:

1. Improved description of software commands
2. How to change sampling rates
3. How to change node addresses
4. Improved description of use and operation:
    - Procedure to turn off the firewall
    - Memory map functions
    - Operating as an administrator (Admin)

Operational Changes to Reduce Power Consumption

Power consumption was reduced to increase battery life as follows:

1. Development of software and firmware to dynamically support the following usage modes:
   - Burst: high-sample rates – 1 kHz to 100 kHz
   - Streaming: actively sampling and transmitting data at < 1 kHz
   - Standby (default): actively waiting for a command – default mode
   - Sleep: periodic sampling of accelerometer with no data storage or transmission when acceleration below defined threshold
   - Deep sleep: sensor is put into a static state a 'no vibration' period of 3 to 12 minutes – dependent on which add-on version is obtained
2. Redesign and reimplement sub-circuit stages, such the oscillator, voltage regulation, and dividers, to reduce power consumption.
3. Development of a deep Sleep operating mode: an electro-mechanical latch-circuit was implemented to allow the sensor to shut-off after being in a static sate for an adjustable time period of 3-12 minutes.

4. Data Collection and Analyses at NTS and Ridgetop Group

Test plans were updated from one to three types of vibration test: (1) fixed frequencies, (2) sweep frequency, and (3) pulse (shock). Testing included tests performed in the Ridgetop lab and external testing at NTS in June of 2017.

NTS Testing

Fixed Vibration Frequencies: Three vibration frequencies at seven levels of force defined and tested: Table 4. The sequences were run at four sampling rates: 160 s/s, 250 s/s, 500 s/s, and 1000 s/s.

Table 4. Fixed Vibration Frequency.

Vibration Frequency: Force
Dwell @ 50 Hz: 5g, 10g, 20, 30g, 50g, 70g, 100g
Dwell @ 100 Hz: 5g, 10g, 20, 30g, 50g, 70g, 100g
Dwell @ 250 Hz: 5g, 10g, 20, 30g, 50g, 70g, 100g

Sweep Vibration Frequency: The sweep frequency as defined as 10 Hz to 500 Hz at two different levels of force: 10g and 40g. The sequences were run at the defined four sampling rates.

Pulse Vibration (Shock): The pulse was defined as a six-millisecond, positive half-sine wave repeated five times at the six different magnitudes of force used for fixed-frequency testing. The sequence was repeated for each of four different sampling rates.

5. Discussion and Results

Ruggedization

No physical damage or anomalies were found during and after the testing regime at NTS. At no time was there any loss of signal.

Improved Signal Quality

After potting and repositioning of components, the signal quality is significantly improved as seen in Figure 14 through Figure 17.

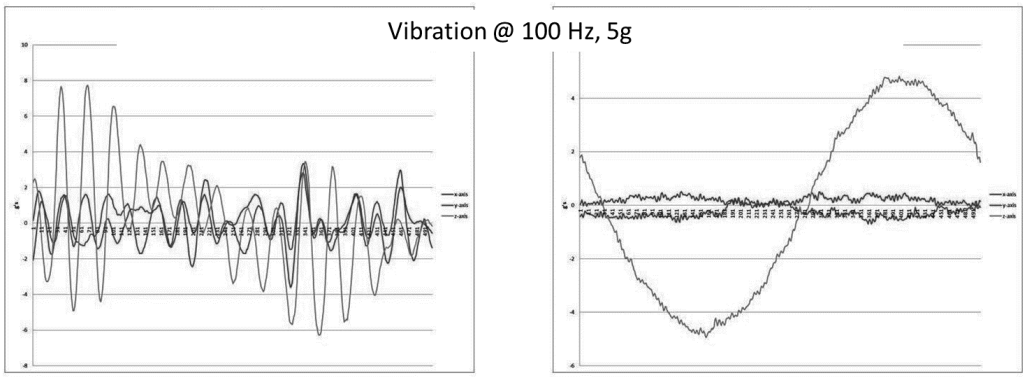

Figure 14: Vibration @ 100 Hz, 5g – Before (Left) and After (Right).

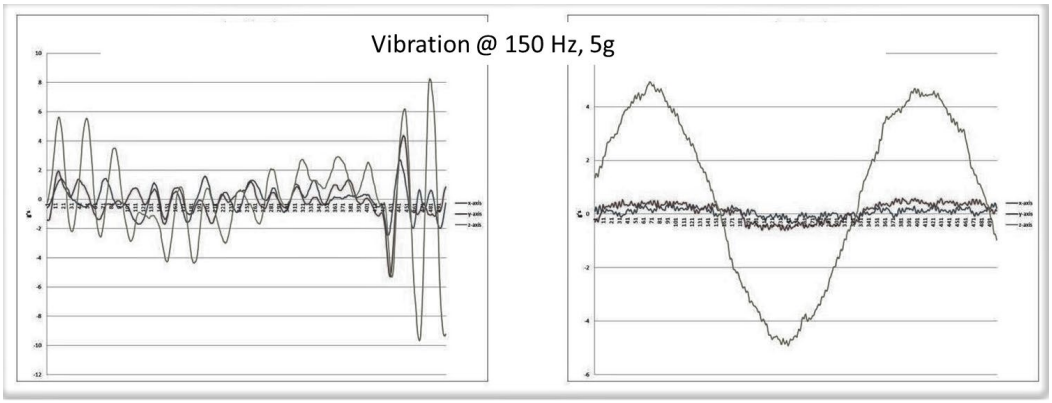

Figure 15: Vibration @ 150 Hz, 5g – Before (Left) and After (Right).

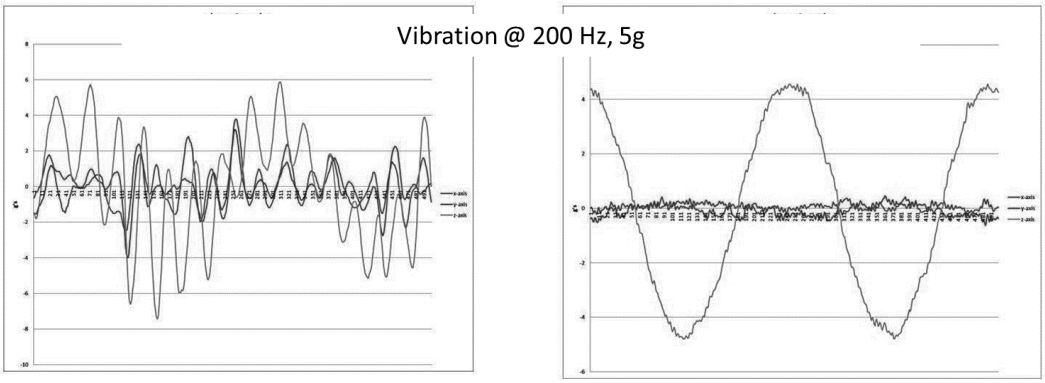

Figure 16: Vibration @ 200 Hz, 5g – Before (Left) and After (Right).

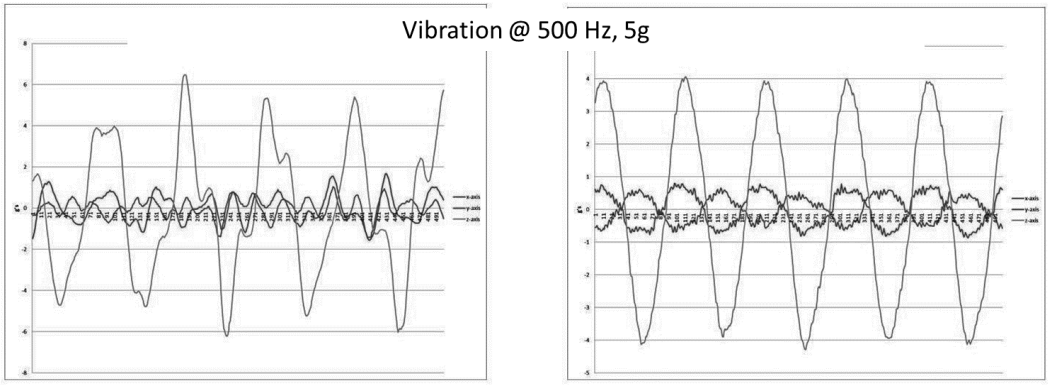

Figure 17: Vibration @ 500 Hz, 5g – Before (Left) and After (Right).

Reduced Harmonic Distortion and Noise, More Accurate Amplitude Measurements: The output signals from the MEMS-based sensor after repositioning and potting of the boards and battery pack no longer exhibit extreme harmonic distortion and noise; the amplitudes more accurately reflect the magnitude of the vibration force; and the bandwidth has been improved from 4-6 Kb/s to 20-22 Kb/s.

Further improvements in signal quality have been made: primarily through improvements in configuring the ground planes, signal paths, and voltage references.

Improved Gateway: A new version of the Gateway for helicopter use is significantly more rugged: (1) it uses super strong Vicor power supply, that went through extensive power cycle testing on the Apache helicopter; and (2) all internal components are compact, soldered to a carrier board, and/or immobilized.

The new Gateway is an Edge Computing, IoT device that taps and processes data where it is generated: increased efficiency, faster transmission, and reduced resources.

NTS - Fixed Frequency:

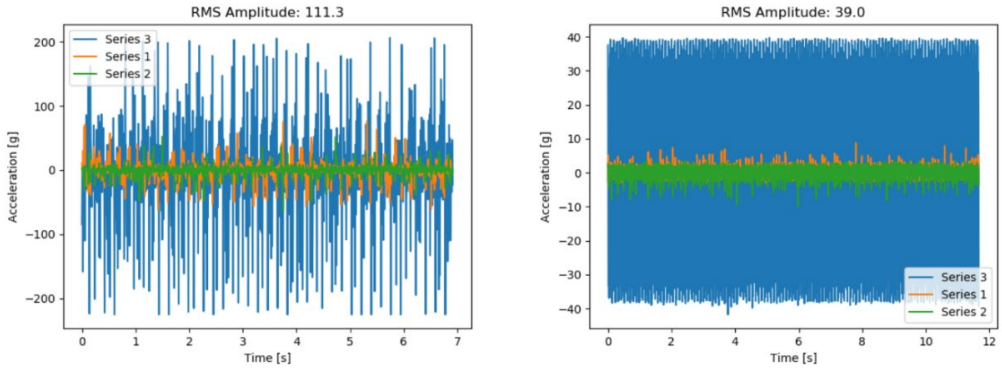

Figure 18: NTS Fixed Frequency Comparison.

NTS Sweep Test - 1 Hz/s Interval, 10 Hz - 250 Hz Frequency Sweep @ 40 g

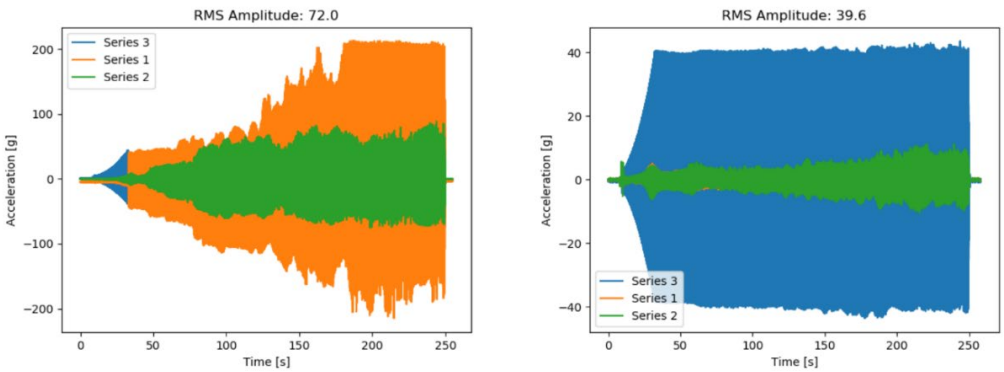

Figure 19: Sweep Frequency Comparison – Non-Potted (Left), Potted (Right).

NTS Shock Test

The non-potted version of the sensor failed during the fixed-frequency and sweep-frequency tests at NTS. The ruggedized (potted) and electrically-improved version of the sensor performed exceedingly well.

Decreased Power – Increased Battery Life

The operational power consumption has been reduced from the levels at the time of the test runs at the NTTC (2015) to those listed in Table 5.

NTS Verification

Ridgetop Group returned to NTS in December of 2017 with a revised test plan that was tailored to the IEC-61373 certification standard. The test conditions were for the body-mounted, bogie-mounted, and axle-mounted categories.

The units under test all survived the testing regime, and provided further repeatability and validation of what was observed in June 2017 with the potted RotoSense design.

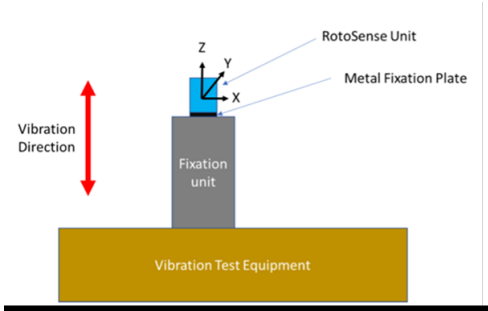

Figure 24 (A): Mounting Configuration of RotoSense™ Unit.

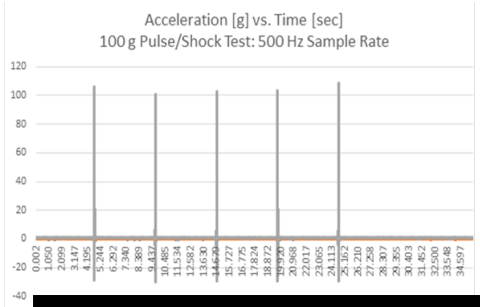

Figure 24 (C): RotoSense output for full shock test (5 sec

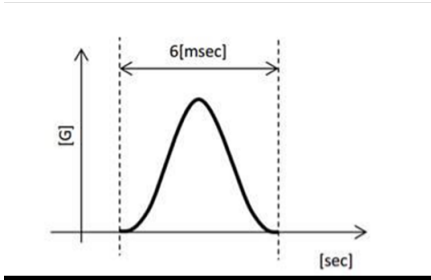

Figure 24 (B): Shock Time Profile (input signal)

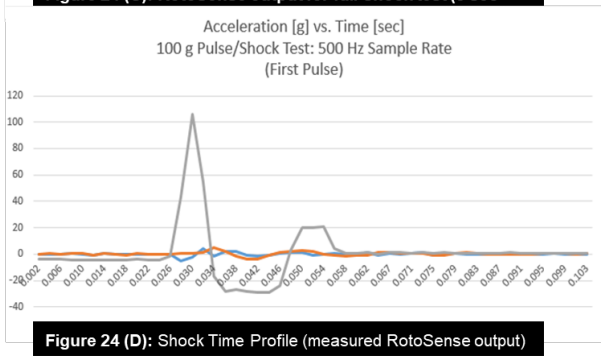

Figure 24 (D): Shock Time Profile (measured RotoSense output)

Figure 20: NTS Results - Shock Test

Table 5: Power Usage (9600 mAh Battery):

Usage Mode	2015	2018
OFF	0	0
Deep Sleep	N/A	< 0.001 mA
Sleep	N/A	< 4.0 mA
Standby	45 – 55 mA	< 22 mA
Streaming	40 – 60 mA	< 25 mA
Burst	45 – 75 mA	< 70 mA sampling < 25 mA data transfer

6. CONCLUSIONS

Prior to the 2018 conference, two versions of MEMS-bases sensors were designed and developed: one version for use in gear boxes of helicopters and the other version for hub mounting on axles of rolling stock. Each version of the sensors, their application, and their testing and results were described and the results evaluated: both versions functioned and operated successfully.

Subsequently, it was discovered that the original RotoSense design for rolling stock was not rugged enough to sustain a customer requirement of applied vibration at 40 g. After

conducting a root cause analysis and research, that version of the sensor was ruggedized by repositioning and potting of the components: the boards and the battery pack. The ruggedized version of the sensor was tested at the National Technical Systems at various regimes: fixed frequency, sweep frequency, and pulse mode vibration at various frequencies and levels of force - no physical failure or anomalies occurred.

Improvement in signal quality (level of harmonic distortion) and the accuracy of measured force were verified by comparing signals from non-ruggedized sensors to those from ruggedized sensors. In addition to ruggedization, improvements were made to the hardware to increase sensor bandwidth and to improve the Gateway with respect to ruggedness, to IoT compatibility, and to communication speeds. Hardware design changes in grounding and signal paths were made to further reduce noise.

The software, firmware, and documentation were updated to increase communication, to reduce timeouts, and to increase functionality and usability.

We achieved a significant decrease in power consumption and a corresponding increase in average battery life. We anticipate further improvements in the future, especially with regards to further reducing power consumption; and we are investigating the feasibility of and approaches to energy harvesting and rechargeable methods to achieve further improvements in extending battery life: enabling design changes have already been developed. In summary:

1. All tested RotoSense units showed high correlation with the input test conditions on the T-1000 shaker.
2. The new RotoSense assembly process demonstrated that it could sustain high [g] operating conditions.
3. The signal to noise ratio was drastically improved, especially when compared to the original assembly.
4. The second trip to NTS provided further validation that the sensor assembly could operate at test conditions similar to that of the IEC-61373 certification standard.
5. The second trip to NTS also validated that the firmware and software enhancements increased data transmission bandwidth and reliability while maintaining high input/output data correlation.

We have designed and developed a third version of RotoSense for embedded planetary gearbox applications. It is the rectangular form factor that was also evaluated with the pinion gear sensor during the NASA project that was embedded in the top half of the gearbox. This particular design does have a 3-axial d-accelerometer instead of a 3-sensor configuration.

Plans are to apply the potting approach to increase the ruggedization of the helicopter version of the sensor. That version has already been improved by increasing the sensor bandwidth, making the Gateway more rugged, and improving Gateway communications.

Acknowledgments

The authors thank Naval Air, Naval Sea, U.S. Army, U.S. Air Force, and NASA research centers for their support and funding of multiple projects that led to the design and development of the prototype solutions and the results described and shown in this paper.

References

[1] Lewicki, D.G., Lambert, N.A., and Wagoner, R.S., (2015) "Evaluation of MEMS-Based Wireless Accelerometer Sensors in Detecting Gear Tooth Faults in Helicopter Transmissions," NASA/TM-2015-218722.

[2] Hofmeister, J.P., Goodman, D., and Wagoner, R. (2016), "Accurate Vibration and Speed Measurement on Rotating Shafts Using MEMS and IoT Single Wireless Triaxle Sensor," Conference of the Society for Machine Failure Prevention Technology, Dayton, OH, 24-26 May, 2016.

[3] Hofmeister, J.P., Pena, W., Wagoner, R., and Nielsen, M., (2017) "Improved RotoSense™ for Rolling Stock: Locomotives and Cars," Conference of the Society for Machine Failure Prevention Technology, Virginia Beach, VA, 16-18 May, 2017.

[4] Lindstrom, M., (2018) "What's Wrong with My Piezoelectric Accelerometer?" PCB-TN-30-0418, MTS Systems Corporation, PCB Piezotronics, Depew, NY, April 2018.